

MODELS FOR THE STRUCTURE AND ORIGIN OF BIPOLAR NEBULAE

MARK MORRIS

Department of Astronomy, Columbia University
 Received 1981 January 26; accepted 1981 April 24

ABSTRACT

The appearance of bipolar nebulae—symmetric reflection nebulae centered on evolved, mass-losing stars—can most simply be accounted for in terms of an axisymmetric distribution of outflowing dust in which the dust is concentrated towards an equatorial plane and declines monotonically with latitude above that plane. The symmetrically placed “horns” that can be seen radiating out of some bipolar nebulae, notably GL 2688, are a natural consequence of such a dust distribution if, at some latitude, the radial optical depth to starlight falls rapidly below unity. Several models of bipolar nebulae are presented; they reproduce well the shapes observed. These structural models for bipolar nebulae lead in turn to an investigation of how such a geometry might arise. Although nonradial pulsation, rotationally forced mass ejection by a single star, and mass loss from a common envelope binary are all considered, the most attractive origin for bipolar nebulae is a binary star system in which the primary is evolving up the red giant branch to the point at which its radius approaches its tidal radius. If this occurs before corotation of the primary with the secondary’s orbit can be achieved, then matter from the primary’s envelope can be gravitationally ejected from the system by the secondary, the ejected material being concentrated toward the system’s equatorial plane, as required. Numerical models of this phenomenon show that gravitational ejection from an asynchronous binary system easily leads to terminal outflow velocities in the observed range (20–50 km s⁻¹), and that the rate of mass loss and the time scale over which the mass ejection takes place are consistent with observations if the particle density in the outer layers of the primary’s atmosphere from which the material is extracted is in the range 10¹⁴–10¹⁵ cm⁻³. If this hypothesis is applicable, bipolar nebulae will probably become planetary nebulae, as previously suggested on observational grounds. It is likely that the central stars of many of the resultant planetary nebulae will be binaries and that the eventual fate of these binaries is to become cataclysmic variables. Thus, bipolar nebulae may represent the phase of extreme angular momentum loss that is needed to account for the small separations of cataclysmic binaries.

Subject headings: interstellar: matter — nebulae: reflection — radiative transfer — stars: binaries

I. INTRODUCTION

Bipolar nebulae are beautiful, symmetric reflection nebulae consisting of dust and molecular gas which appear to be expanding away from a central star. Their axisymmetric appearance is determined by the concentration of the outflowing gas and dust toward an equatorial plane. The dust in and near the equatorial plane is opaque and blocks visual light from the central star, whereas in the polar (axial) directions, starlight is scattered by the dust but suffers only a moderate amount of extinction. The emerging optical emission is thus concentrated toward the two polar directions and is symmetric about the polar axis. The evolutionary status of bipolar nebulae as a group has been examined by Calvet and Cohen (1978), who conclude that most bipolar nebulae are objects which are in the early stages of the formation of planetary nebulae.

In this paper, I propose a model in which the envelopes of bipolar nebulae result from mass lost from close binary systems (separation 0.2–10 AU), as the primary evolves up the red giant branch. In the preferred model, the secondary pulls matter from the primary atmosphere as the primary approaches its tidal radius and flings that matter out of the system. The ejected matter is concentrated towards the system’s equatorial plane, as is required to explain the geometry of bipolar nebulae. Furthermore, this process carries angular momentum out of the system and thus permits the system to evolve quickly to a new configuration as the secondary spirals toward the primary.

The known characteristics of bipolar nebulae are summarized in § II. It is argued that observations to date of bipolar nebulae are consistent with a dust and gas distribution that decreases monotonically with latitude above the equatorial plane. In § III, the details of

the proposed mass ejection mechanism are presented, including the results of numerical three-body calculations which simulate that mechanism both with and without stellar pulsation. The ultimate fate of a bipolar nebula depends on, among other things, the mass ratio and the initial separation. With appropriate initial conditions, bipolar nebulae can be the logical precursors of common envelope binaries, planetary nebulae, and cataclysmic binaries. This is discussed in § IV. Finally, the conclusions of this work and suggestions for further study are summarized in § V.

II. CHARACTERISTICS OF BIPOLAR NEBULAE

In astronomical literature, the terms “bipolar nebula” and “biconical nebula” have both been used to refer to at least two different types of objects. The first type is a circumstellar envelope which is in expansion about a presumably evolved star. Being an evolved object, this first type is, in general, relatively isolated and not associated with interstellar clouds. This is the type with which this paper is concerned. The second type of bipolar or

biconical nebula appears to be intimately associated with interstellar molecular clouds, and is therefore likely to be a young object, possibly an accretion disk surrounding a newly formed star which may have a substantial T Tauri-like wind. In this case, the nebula may be either an H II region or a reflection nebula. Examples of the second type of nebula are S106 (Pismis and Hasse 1980; Solf 1980) and R Mon (Stockton, Chesley, and Chesley 1975). I suggest that in order to avoid an ambiguous nomenclature for these objects, the first type be referred to only as bipolar nebulae and the second type only as biconical nebulae.

Bipolar nebulae (hereafter BPNs) are not very common objects. The total number of BPNs recognized as such is only ~ 12 , and this includes objects at distances up to several kpc. Infrared and H α surveys have probably located a large fraction of BPNs within 1–2 kpc of the Sun, and in spite of occasional serendipitous discoveries of more distant BPNs (such as was the case with OH 231.8+4.2), most nearby BPNs with large mass loss rates have probably been accounted for. The known BPNs are listed in Table 1 along with references for

TABLE 1
LIST OF BIPOLAR NEBULAE

Name (1)	Spectral Type of Central Star (2)	Envelope Chemistry (3)	References (4)
M 1–92 (Minkowski's Footprint) ... HD 44179	B0.5–1 V	O	1, 2, 3, 4, 5
(Red Rectangle)	B9–A0 III	?	6, 7, 8
GL 618	O9.5–B0	C	9, 10, 11, 12
GL 2688	F5 Ia	C	3, 5, 7, 10 13, 14, 15, 16
Mz 3 (PK 331–1°1, VV 80)	O9.5–B0	?	17, 18
OH 231.8+4.2 (OH 0739–14)	M6 I	O	4, 19, 20, 21
Roberts 22 (OH 284.2–0.8)	A2 Ie	O	22, 23, 24
He 401	Be!	?	25
GL 2789 (V645 Cyg)	O7–O9 V or A5e	O	26, 27, 28
ESO–172(1242–54.2) (Boomerang Nebula)	G0 III	?	29, 30
M 2–9 (MH α 362–1, Butterfly Nebula)	B1	?	11, 12, 31, 32
M 1–91	B0 or earlier	?	11

REFERENCES—(1) Minkowski 1946. (2) Herbig 1975. (3) Cohen and Kuhl 1977. (4) Morris and Bowers 1980. (5) Schmidt, Angel, and Beaver 1978. (6) Cohen *et al.* 1975. (7) Jones and Dyck 1978. (8) Schmidt, Cohen, and Margon 1981. (9) Westbrook *et al.* 1975. (10) Lo and Bechis 1976. (11) Calvet and Cohen 1978. (12) Schmidt and Cohen 1981. (13) Ney *et al.* 1975. (14) Crampton, Cowley, and Humphreys 1975. (15) Zuckerman *et al.* 1976. (16) Shawl and Tarengi 1976. (17) Cohen *et al.* 1978. (18) Glass and Webster 1973. (19) Turner 1971. (20) Cohen and Frogel 1977. (21) Allen *et al.* 1980. (22) Roberts 1962. (23) Manchester, Goss, and Robinson 1969. (24) Allen, Hyland, and Caswell 1980. (25) Allen 1978. (26) Cohen 1977. (27) Humphreys, Merrill, and Black 1980. (28) Harvey and Lada 1980. (29) Wegner and Glass 1979. (30) Taylor and Scarrott 1980. (31) Allen and Swings 1972. (32) van den Bergh 1974.

their identification. Of these objects, GL 2789 has an uncertain classification as a BPN. It appears to be associated with an extended molecular cloud (Harvey and Lada 1980) and may therefore be a young object. Also, its optical appearance lacks the symmetry of other BPNs (Cohen 1977). Some BPNs (M 2-9, for example; Aller and Liller 1968) have been placed in the class of planetary nebulae. This presumably reflects the evolutionary continuity between BPNs and planetary nebulae (Calvet and Cohen 1978). Therefore, some of the BPNs in Table 1, M 2-9, M 1-91, and Mz 3, might best be regarded as transition objects—late BPNs or early planetaries. Also, GL 618 has been described as a pre-planetary (Westbrook *et al.* 1975).

The lifetimes of BPNs are ≥ 1000 years. This time is the expansion time scale for the envelope of OH 231.8+4.2, which has a minimum diameter of $\sim 3 \times 10^{17}$ cm and an expansion velocity of 50 km s^{-1} (Morris and Bowers 1980). The minimum expansion times of M 1-92 and GL 2688 are about $3-4 \times 10^3$ years, as judged by their estimated distances of 3 kpc and 1.5 kpc, respectively (Cohen and Kuhl 1977), their maximum optical extents ($12''.5$ and $30''$, respectively) (Herbig 1975; Ney *et al.* 1975), and their outflow velocities of 19 and 15 km s^{-1} , respectively (Davis, Seaquist, and Purton 1979; Zuckerman *et al.* 1976). The expansion times of other BPNs are probably similar. The low space density of BPNs (\lesssim a few per kpc^3) is consistent with a relatively short lifetime of a few thousand years if a fair fraction (perhaps ~ 0.1) of all stars pass through the BPN stage.

Column 2 of Table 1 lists the inferred spectral types of the central stars of BPNs. Since the central stars are usually hidden by dust, these types were deduced indirectly from highly reddened colors or from spectra of the starlight reflected in the polar nebulae. They are therefore subject to some uncertainty. Even so, it is clear that the spectral types vary widely among BPNs.

In many cases, the gaseous envelopes of BPNs can be detected in the radio spectral lines of molecules. The radio spectra permit a distinction between carbon-rich and oxygen-rich envelope chemistry. Oxygen-rich envelopes, by analogy with the envelopes around many oxygen-rich Mira variables and M supergiants, often display maser emission from OH and H_2O (Davis, Seaquist, and Purton 1979; Morris and Bowers 1980; Allen, Hyland, and Caswell 1980) and have weak or undetectable CO emission, whereas carbon-rich BPN envelopes, by analogy with the envelopes around a number of carbon stars (Zuckerman *et al.* 1977, 1978), display quasi-thermal emission at millimeter wavelengths from a number of molecules, including CO (Lo and Bechis 1976), HCN, CS, and HC_3N (Zuckerman *et al.* 1976). The envelope chemistry of BPNs, as inferred in this way, is listed in column 3 of Table 1. The molecular emission lines from BPNs are broad (40-100

km s^{-1}), indicating that these nebulae are rapidly expanding (Zuckerman *et al.* 1976; Lo and Bechis 1976; Morris and Bowers 1980; Davis *et al.* 1979; Allen, Hyland, and Caswell 1980). In addition, Morris and Bowers (1980) have argued that the OH maser line shapes observed toward OH 231.8+4.2 and M 1-92 can be accounted for if the maser arises in an expanding envelope which is concentrated towards an equatorial plane, assuming that the Earth is not located near that plane. The OH maser line shapes from Roberts 22 (Allen, Hyland, and Caswell 1980) can readily be accommodated by the same geometry (cf. Fig. 7 of Morris and Bowers 1980).

Since most of the mass in BPNs is optically invisible, the optical observations provide little information on masses. However, the nebular masses can be roughly estimated from the infrared, millimeter, and maser observations. Thus, OH 231.8+4.2 appears to have a nebular mass of $0.01-0.1 M_\odot$ (Allen *et al.* 1980; Morris and Bowers 1980), which leads to a mass loss rate of 10^{-4} to $10^{-5} M_\odot \text{ yr}^{-1}$. The mass loss rate of GL 2688 has been estimated at $3 \times 10^{-5} M_\odot \text{ yr}^{-1}$ (Lo and Bechis 1976; Morris 1980). These two rates probably represent the upper extreme of the known BPNs; the other objects have been studied in less detail because they are weaker infrared or radio sources.

Although the terminal outflow velocities in BPNs are relatively high, much higher velocities on the order of $400-600 \text{ km s}^{-1}$ occur in some of these (M 1-92 [Herbig 1975] and GL 2789 [Cohen 1977]) as evidenced by P Cygni profiles of some of the emission lines. In addition, the $\text{H}\alpha$ line of Roberts 22 shows a plateau of emission extending over 600 km s^{-1} (Allen, Hyland, and Caswell 1980). These extremely high velocities probably occur very near the stellar surfaces and are possibly due to a stellar wind from the central object (cf. § III).

Polarization studies of BPNs have consistently shown a large percentage polarization—so large, in fact, that it has been argued that the nebulae are dominated by singly scattered photons from a central source (e.g., Schmidt, Angel, and Beaver 1978). Since the reflection nebulosity usually appears at high latitudes ($\gtrsim 50^\circ$) above the equatorial plane, the nebula as a whole displays a polarization angle which is perpendicular to the nebular axis (Cohen *et al.* 1975; Westbrook *et al.* 1975; Ney *et al.* 1975; Cohen and Kuhl 1977; Jones and Dyck 1978; Kobayashi *et al.* 1978; Schmidt, Angel, and Beaver 1978).

The results of the optical and infrared studies of BPNs quoted in Table 1 are consistent (with the possible exception of GL 2789) with an axisymmetric geometry having reflection symmetry about an equatorial plane. Furthermore, the observations suggest that the dust density is a decreasing function of the latitude above that equatorial plane. Under this hypothesis, the reflection nebula becomes apparent at high enough latitudes

that the radial optical depth through the dusty envelope is less than or about equal to unity. To demonstrate that this is a viable hypothesis, we construct model reflection nebulae assuming that the decrease of density with latitude, θ , is given by a function $f(\theta)$. If the outflow velocity is constant, the dust density as a function of θ and radius, r , is thus

$$n_d(r, \theta) = k f(\theta) / r^2, \quad (1)$$

where k is a constant. If the optical depth (assumed independent of wavelength for simplicity) is related to the dust density by $d\tau_d = c n_d d\xi$, where c is a second constant and ξ is the distance through the medium, then the radial optical depth from the inner boundary of the dust envelope, r_0 , out to radius r is

$$\tau_d(r, \theta) = ck f(\theta) (1/r_0 - 1/r). \quad (2)$$

For the sake of simplicity in this merely illustrative argument, I assume that only single scatterings are important and that the scattering is isotropic. Then the intensity of light scattered at (r, θ) is

$$dI(r, \theta) = \frac{F_*}{4\pi} \left(\frac{r_*}{r} \right)^2 cA n_d(r, \theta) \exp[-\tau_d(r, \theta)], \quad (3)$$

where F_* is the intensity at the stellar surface, r_* is the radius of the central star, and A is the dust grain albedo. The emergent intensity along a line of sight from the reflection nebula is obtained by integration of equation (3) along that line of sight through the axisymmetric nebula. If z is the distance variable along the line-of-sight dimension, then the emergent intensity is proportional to

$$\int_{-\infty}^{\infty} \frac{dz f[\theta(z)]}{r(z)^4} \exp \left[-ck \left\{ f[\theta(z)] \left(\frac{1}{r_0} - \frac{1}{r(z)} \right) + \int_{-\infty}^z \frac{dz' f[\theta(z')]}{r(z')^2} \right\} \right]. \quad (4)$$

The last term in the exponential accounts for absorption of the scattered light along the line of sight by intervening dust. The functions $\theta(z)$ and $r(z)$ depend on the observer's latitude, θ_0 , and on where the line of sight intersects the nebula. If the line of sight passes through the nebula at a point on the sky (x, y) , where y is the projected distance from the central star along the polar axis and x is the distance perpendicular to that axis,

then

$$r(z) = (x^2 + y^2 + z^2)^{1/2}$$

$$\theta(z) = \sin^{-1} [(y \cos \theta_0 - z \sin \theta_0) / r(z)]. \quad (5)$$

The function $f(\theta)$ was chosen to be

$$f(\theta) = \exp(-\theta/\theta_1) \{ \tanh[(\theta_2 - \theta)/\sigma] + 1 \}. \quad (6)$$

The exponential ensures a monotonic decrease, while the function in brackets allows for a cutoff in density at some latitude θ_2 .

Model nebulae which were constructed using equations (4)–(6) are shown in Figures 1a–1d. In all cases, the observer is located in the equatorial plane ($\theta_0 = 0^\circ$), and therefore only one of the two symmetrical lobes is shown. Clearly, there is some variety possible in the appearance of BPNs, and the possible forms encompass those that are observed. The trend in Figures 1a–1d is due primarily to a decreasing cutoff latitude, θ_2 . This treatment ignores multiple scattering of photons, so one should expect the true shapes of the reflection nebulosity isophotes to deviate somewhat from those shown. However, Schmidt, Angel, and Beaver (1978) argue that multiple scattering is not very important for most of the light in a few BPNs.

Figure 1b indicates that “horns” may appear in some nebulae. This happens when the dust density falls off rapidly with latitude. The orientation of the horns indicates at which latitude the radial optical depth has dropped below unity. When $\tau(r, \theta) \sim 1$, the maximum amount of starlight is scattered out of the nebula. At lower latitudes light cannot penetrate the dust to be scattered in the outer parts of the nebula, and at higher latitudes the dust density is so low that only a fraction of the light is scattered. Horns of just this nature are seen in both lobes of GL 2688 (Ney *et al.* 1975). The fact that GL 2688 has slightly more bulbous lobes than are indicated by Figure 1b can probably be attributed to the importance of forward scattering and to the multiple scattering which must take place in those directions for which $\tau(r, \theta) \gtrsim 1$. Figure 1d bears some resemblance to Mz 3 (Cohen *et al.* 1978) and the Red Rectangle (Cohen *et al.* 1975), when one allows for forward and multiple scattering.

The function chosen to model the latitude distribution of density (eq. [6]) is arbitrary. The important feature for producing realistic looking bipolar nebulae is that the density fall off rapidly with θ at some θ . In the dark, optically thick part of the envelope near the equatorial plane, the density of dust is constrained only to be greater than in the reflection nebula.

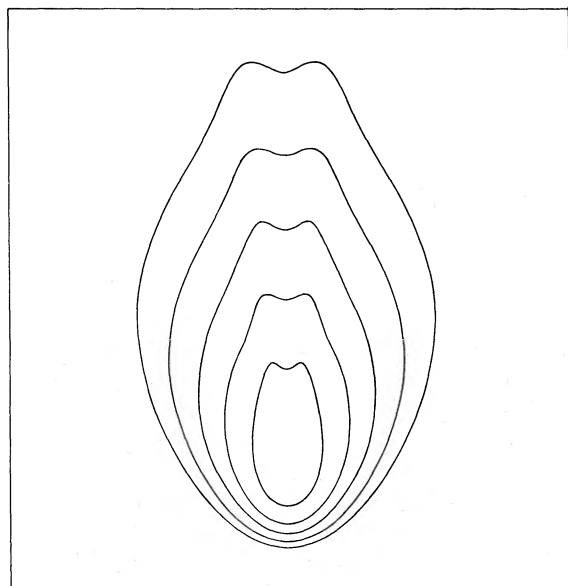


FIG. 1a

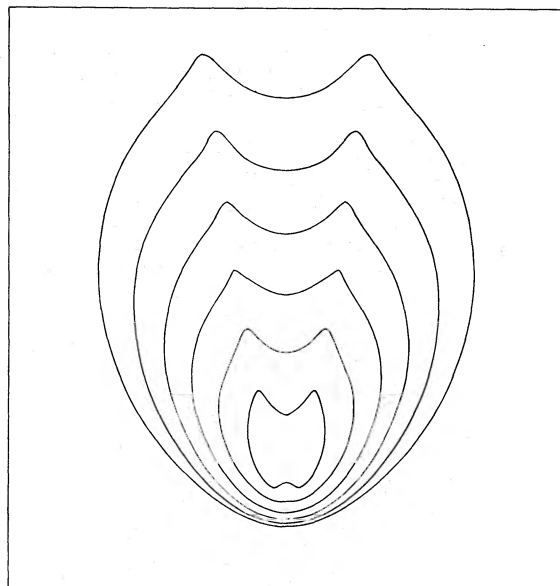


FIG. 1b

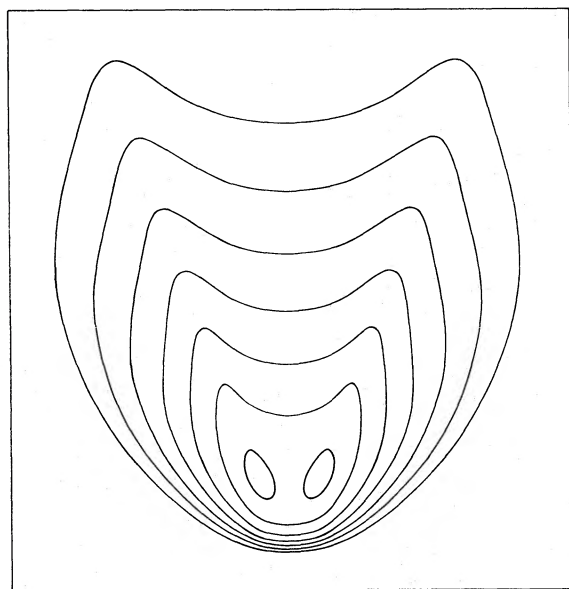


FIG. 1c

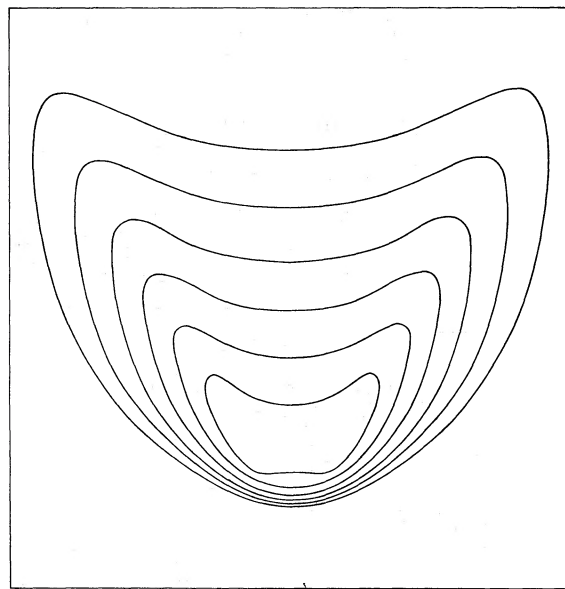


FIG. 1d

FIG. 1.—Isophotes of model bipolar nebulae constructed according to eqs. 4–6 in text. The observer's latitude is taken to be 0° , and because of the symmetry at this latitude, only one lobe is shown. In all cases, the isophotes are separated by one-half-magnitude intervals, the scaling factor ck/r_0 is 8, and the vertical extent of the outer contour is approximately $y=10r_0$. The parameters characterizing each model are: (a) $\theta_1=50^\circ$, $\theta_2=84^\circ$, $\sigma=4^\circ$; (b) $\theta_1=40^\circ$, $\theta_2=80^\circ$, $\sigma=2^\circ$; (c) $\theta_1=35^\circ$, $\theta_2=70^\circ$, $\sigma=4^\circ$; (d) $\theta_1=30^\circ$, $\theta_2=60^\circ$, $\sigma=6^\circ$.

III. THE MASS LOSS MECHANISM

There are three conceivable situations which might give rise to the quasi-planar, axisymmetric geometry of the expanding envelopes of bipolar nebulae. These are: (1) ejection by large-amplitude, nonradial pulsations of a single star, (2) rotationally forced mass ejection from a single star, and (3) mass ejection from a binary system.

The first of these possibilities was suggested by Schmidt, Angel, and Beaver (1978). They envisioned an oscillation in which the star is alternately oblate and prolate, and in which matter escapes at the radial extremes of each half-cycle. Thus, in the oblate phase, matter is ejected in the equatorial disk and becomes the dark, optically thick component, while in the prolate phase, matter is ejected along the poles and becomes the reflection nebula. The resulting latitudinal distribution of matter would violate the above contention that the dust density is a monotonically decreasing function of latitude. In particular, given this model, one would expect to see a second reflection nebula at the optically thin surface of the equatorial disk—this would cause the optical appearance of BPNs to be more complex than they in fact appear to be. Although purely pulsational mechanisms of mass ejection in BPNs cannot be ruled out altogether, they are unattractive in view of the absence of any known nonradial mode of large amplitude which could conceivably cause mass ejection in the manner observed for BPNs. Such mechanisms will therefore not be considered further in the discussion which follows.

Rotationally forced mass ejection by a single star was considered by Mufson and Liszt (1975) in order to account for line profiles from the envelope of the carbon star CIT 6¹. Their model applies to an extremely rapidly rotating red giant in which the mean turbulent velocities are quite large (5–10 km s⁻¹). In such a model, marginally bound gas near the stellar equator can achieve the escape velocity, but the terminal velocity is likely to be quite small for realistic cases. No analogous model is applicable to BPNs because the emitting gas in these objects has achieved a relatively large terminal velocity. In addition, the outflow velocity in BPNs is not a strong function of latitude (compare the optically determined velocities in M 1–92 [Herbig 1975] with those implied by the OH maser [Davis, Seaquist, and Purton 1979; Morris and Bowers 1980]) as it would be if the mass were ejected by rotation of a single star.

In order to achieve outflow velocities up to 50 km s⁻¹ and outflow rates of 10⁻⁵ M_⊙ yr⁻¹, I conclude that the mass-losing object is most likely to consist of more than a single star. If the central stars of BPNs are (or were originally) binaries, I find two possible scenarios for the mass ejection mechanism occurring, respectively, before

¹An alternative explanation of these line profiles has since appeared (Morris 1980).

and after the binary evolves into contact. These are (1) the gravitational ejection of matter from the extended atmosphere of the primary as it evolves up the red giant branch for the first time and expands past its tidal radius, and (2) mass loss from the envelope of a common envelope binary. Each of these is discussed separately below.

a) *Mass Loss from a Common Envelope Binary*

The current picture of binary star evolution is one in which the system evolves peacefully to the common envelope stage. It does this by transfer of the secondary's angular momentum to the primary through tidal and/or dynamical friction until corotation of the primary envelope is achieved, followed by transfer of matter to the secondary until the secondary's Roche lobe is filled, and finally by continued expansion of the primary until the system's outer Roche lobe is filled (e.g., Paczynski 1971, 1976). In a common envelope binary, there are three conceivable mechanisms by which mass can be lost from the system.

The first is by acceleration of matter outward from the outer Lagrangian point, L_2 (Kuiper 1941; Ritter 1976; Flannery and Ulrich 1977; Flannery 1977; Shu, Lubow, and Anderson 1979). This mechanism requires that material at L_2 corotate with the binary, although the validity of this assumption is subject to some question (Paczynski 1976; Shu *et al.* 1979; Meyer and Meyer-Hofmeister 1979). At first sight, this is an attractive mechanism because the ejected matter flows outward in a plane and can achieve rather large escape velocities. However, the time scale for this mechanism to operate appears to be too short because the mechanism is unstable. Matter ejected from L_2 has a large specific angular momentum (Flannery and Ulrich 1977), and therefore the angular momentum lost from the system drains the orbital angular momentum of the binary. The binary separation thus decreases, causing L_2 to move inwards and more of the envelope (that external to L_2) to be ejected. The time scale for this phase of rapid dissipation of the binary's envelope and angular momentum (estimated to be $\lesssim 10$ years by Flannery and Ulrich 1977) is probably much less than the expansion times of BPNs. However, if the secondary is not corotating with its orbital motion, or if there are large scale flows in the common envelope (e.g., Shu, Lubow, and Anderson 1979), then mass loss from L_2 might be inhibited, and the process might therefore be lengthened. On the other hand, this might equally well lead to a non-corotating common envelope from which mass loss does not occur until further evolution has taken place and the envelope has expanded considerably. An important observational objection to mass loss from L_2 as an explanation for BPNs is that it would give rise to only a very thin expanding disk of outflowing material rather than to the observed mass outflow in BPNs where a substantial

amount of material appears at high latitudes. Even if this mechanism could eject matter over a large range of latitudes, it would probably result in a terminal velocity that varies strongly with latitude, contrary to the observations of M 1-92.

The second possible mass loss mechanism appears when the binary system has evolved even further. If the envelope is not lost by mass ejected at L_2 , then the common envelope is presumably not corotating and the separation of the cores of the two stars decreases as the stars yield their angular momentum to the envelope through viscous interaction. The angular momentum and orbital energy deposited in the envelope cause the envelope to expand and distend into a highly oblate configuration. This is a conceivable situation for relatively slow mass loss to occur in the manner of Mufson and Liszt (1975), since the common envelope would be loosely bound and have rather large convective velocities. This mechanism appears to meet the same observational objections as does mass loss from L_2 , but it cannot be ruled out until models containing all the important physical processes are constructed. Calculations by Taam, Bodenheimer, and Ostriker (1978) and by Meyer and Meyer-Hofmeister (1979) show that in a few models the envelope is otherwise dynamically stable until the stellar cores are quite close, at which point the orbital energy deposited in less than a convection time scale can in some cases eject the entire envelope explosively. This third ejection mechanism is much too fast to account for BPNs.

In sum, it appears that mass loss from a common envelope binary can conceivably account for BPNs, although the mechanisms considered here may have difficulties with the observational constraints. However, much remains to be learned before this possibility can be properly assessed. In this section, it has been assumed that the primary's envelope is not lost before a contact system is established. The ideas and calculations presented in the following section suggest that this might not be a good assumption for some binary systems.

b) Mass Lost Prior to Contact

It is possible for matter to be gravitationally ejected from a separated binary system if material from the primary is levitated beyond the primary's tidal lobe, and if the primary's rotation is not near synchronism. If the system has somehow been brought to nearly synchronous rotation, then mass ejection is unlikely because levitated matter will tend to fall onto the secondary rather than be ejected, and a common envelope binary can result. But if a substantial fraction of the available angular momentum is lost to ejected matter during the orbital evolution of the binary, then synchronism is not easily achieved, and mass loss will continue until the stars merge or until the primary is finally brought into corotation.

In the absence of mass ejection, synchronization is inevitable unless the binary separation is greater than several times the primary radius, or unless the binary's mass ratio is ≥ 6 . As the primary expands in its evolution up the red giant branch, its radius eventually reaches \sim one-third to one-half of the binary separation. Somewhere near that point, the time scale for transfer of the orbital angular momentum into rotational angular momentum of the primary by tidal interaction becomes comparable to or less than the expansion time scale for the primary. Therefore, unless the secondary's mass (M_s) is less than \sim one-sixth of the primary's mass, M_p , the primary will eventually be brought into corotation (Sparks and Stecher 1974; see also Meyer and Meyer-Hofmeister 1979). The estimate of the synchronization time scale is based on a calculation in which turbulent viscosity retards the equilibrium tide (Alexander 1973; see also Scharlemann 1981), but which assumes small deviations from synchronism, so it may not be the appropriate synchronization time for a red giant which starts with almost zero angular velocity. In that case, the tidal friction might be dominated by the dynamical tide (e.g., Zahn 1975, 1977). In either case, the synchronization time scale is rather uncertain, but it is probably not greatly longer than assumed above. If $M_p/M_s \geq 6$, then the binary will always remain asynchronous (Sparks and Stecher 1974).

If gravitational mass ejection (described below) sets in before synchronism is reached, it drains the secondary's angular momentum and can retard the synchronization process considerably, depending on the rate of mass ejection. As a result, mass ejection becomes a contributing factor to further mass ejection. Furthermore, in the presence of mass loss, the mass ratio M_p/M_s above which synchronism can never be achieved is decreased to a value smaller than 6.

Gravitational ejection from an asynchronous binary is the most attractive model of all those considered in this paper for mass ejection leading to bipolar nebulae. In order to explore this model in some detail, I have performed numerical calculations which yield orbits simultaneously for a large number of negligible-mass particles in the gravitational field of a binary system (i.e., the restricted three-body problem). The particles are originally placed so as to cover a spherical surface which represents the outer layers of the primary atmosphere (in general, this surface is not to be identified with the photosphere). The primary is assumed to be undergoing both orbital motion and solid-body rotational motion. The original velocity of each particle is therefore specified to be the instantaneous velocity of the point on the rotating, spherical surface on which the particle sits.

The subsequent motion of all particles is followed in the nonrotating frame of reference as a result of the gravitational forces of the two stars. The surface density

of particles on the original particle surface is kept constant by replacing particles which are pulled away from their original sites on that surface with newly created particles. If the distance of a particle from the system's center of mass exceeds five times the binary separation, and if the particle's total energy is positive, it is considered to have escaped, and its terminal velocity (i.e., its asymptotic velocity at large distances from the binary) is stored for later averaging.

Hydrodynamical effects are not explicitly included in these primarily dynamical calculations, although in collisions between particles they clearly cannot be ignored. The particles are assumed to have a finite size equal to their original separations on the primary surface (see Appendix for details). From a hydrodynamical point of view, the expected gas densities in the material constituting the particles are large enough (10^{11} – 10^{15} cm $^{-3}$) that particles which collide with each other will dissipate most of the kinetic energy of their relative motion. Therefore, one would expect colliding particles (or gas streams) essentially to merge and then expand at the sound speed. However, the expected sound speeds of a few km s $^{-1}$ are much smaller than the space velocities of the particles, so that a particle would not expand greatly during the time scale for its dynamical motion in the binary system. Therefore, in the dynamical calculations reported here, we hold the particle size constant and make the approximation that when two particles collide (i.e., when their centers move to within 0.6 particle diameters), they are merged into a single particle in such a way that the merged particle carries the combined mass and linear momentum of the colliding pair. In a crude sense, the merging of particles is analogous to the inclusion of a strong viscous interaction between adjacent or colliding gas streams.

The model is symmetric about the equatorial plane, and consequently the particle orbits are followed in one hemisphere only. As a result of this symmetry, an important effect of the assumption that colliding particles are merged is that whenever a particle crosses the midplane, it meets its symmetric counterpart from the opposite hemisphere. (Again from a hydrodynamical point of view, this behavior translates into a strong midplane shock because of the highly supersonic velocities with which particles approach the midplane). The merged particle which results moves thereafter in the midplane, since the total vertical momentum before and after the collision is zero. Because the vertical component of force is always toward the midplane, all particles which leave the primary surface either begin in the midplane or are destined to end up in it. The asymptotic mass outflow in this symmetric model is therefore confined to a plane. Calculations based on the other extreme, that in which particles are not merged and may pass unhindered through the midplane, show that matter is ejected at all latitudes (though seldom, if ever, at latitudes near 90°),

with a marked concentration towards the midplane. The realistic situation is somewhere in between, since asymmetries are probably present in the primary atmosphere and thus in the gas flow, so that not every gas stream will have a symmetric counterpart. This is discussed further below. Since we are concerned here with mass loss rates and the terminal velocities rather than with the latitude distribution, the completely symmetric model suffices for demonstrative purposes.

The calculations reported here include no evolutionary effects (i.e., no change in the binary separation as a result of angular momentum loss, and no change in the secondary radius as a result of accretion). They are therefore meant for an instantaneous examination of the dynamics of a binary system. Evolution is clearly important, and, if BPNs are a guide, rapid. However, because the evolution depends upon the unknown density at the particle surface, it is premature to present calculations which follow the evolution in detail. Further particulars on the method of calculation are presented in the Appendix.

The results of the numerical calculations show that mass loss is readily accomplished if the ratio of the binary separation to the radius of the original particle surface is in the range 1.0–1.5. There is a variety of possible trajectories for particles which attain the escape velocity, but in most cases they are pulled out of the surface and given a single, radially directed impulse as they move towards, and then behind, the orbiting secondary. On a large scale, the outflowing material takes the form of an expanding spiral which begins just behind the secondary and which soon loses its definition as successive density maxima spread out and merge.

A summary of the numerical results is shown in Table 2, which presents a number of models having various values of the mass ratio of the binary (col. 1), of the radius of the original particle surface around the primary (col. 2), and of the binary separation (col. 3). In all models the mass of the primary is taken to be $2.5 M_{\odot}$. The assumed rotational angular velocity of the primary is expressed in column (4) as a fraction, Ω , of the binary's orbital angular velocity. Thus $\Omega=1$ for synchronism. The effects of pulsation were investigated in some models by invoking a sinusoidal variation in the radius of the original particle surface about the equilibrium radius given in column (2) (see Appendix for details). The amplitude of the oscillation is expressed in column (5) as a fraction, δ , of the equilibrium radius. The results of the models are summarized in columns (6)–(10). Column (6) shows the terminal velocity, V_T , of ejected matter. The rate of mass loss from the system is given in column (7) in terms of n_H , the number density of hydrogen nuclei (in cm $^{-3}$) at the original particle surface. The ratio of mass transferred to the secondary to the mass ejected from the system, per unit time interval, is listed in column (8). Column (9) shows the ratio, R , of

TABLE 2
CHARACTERISTICS OF NUMERICAL MODELS OF MASS LOSS FROM CLOSE, ASYNCHRONOUS BINARIES

Mass Ratio (1)	Radius of Particle Surface (10^{13} cm) (2)	Binary Separation (10^{13} cm) (3)	Ω (4)	δ (5)	V_T (km s^{-1}) (6)	\dot{M} ($M_{\odot} \text{ yr}^{-1}$) (7)	M transferred M ejected (8)	R (9)	τ (yr) (10)
3 ...	1	1.6	0.0	0	...	0	...	0	$1.3 \times 10^{18}/n_H$
3 ...	1	1.6	0.5	0.1	...	0	...	0	$(2.4 \times 10^{18}/n_H)$
3 ...	1	1.5	0.3	0.1	29.5	$7.9 \times 10^{-20} n_H$	23.4	+5.45	$1.9 \times 10^{18}/n_H$
3 ...	1	1.4	0.6	0.1	14.2	$3.4 \times 10^{-20} n_H$	107.0	-0.15	$(9.8 \times 10^{17}/n_H)$
5 ...	1	1.3	0	0	38.7	$7.2 \times 10^{-21} n_H$	15.2	+0.02	$2.9 \times 10^{17}/n_H$
5 ...	1	1.25	0	0	30.5	$3.0 \times 10^{-19} n_H$	0.68	+1.03	$1.9 \times 10^{17}/n_H$
5 ...	1	1.25	0.1	0	30.7	$4.5 \times 10^{-19} n_H$	1.55	+2.11	$1.8 \times 10^{17}/n_H$
5 ...	1	1.25	0.2	0	25.7	$4.2 \times 10^{-19} n_H$	3.63	+3.74	$2.3 \times 10^{17}/n_H$
5 ...	1	1.25	0.3	0	25.0	$2.6 \times 10^{-19} n_H$	8.88	+4.40	$3.9 \times 10^{17}/n_H$
5 ...	1	1.25	0.4	0	21.0	$2.3 \times 10^{-19} n_H$	13.1	-64.0	$5.6 \times 10^{17}/n_H$
5 ...	1	1.25	0.5	0	15.6	$2.3 \times 10^{-19} n_H$	14.8	-2.63	$9.8 \times 10^{17}/n_H$
5 ...	1	1.25	0.6	0	18.7	$1.1 \times 10^{-19} n_H$	42.3	-0.55	$(1.2 \times 10^{18}/n_H)$
5 ...	1	1.20	0	0	22.2	$4.2 \times 10^{-19} n_H$	0.19	+1.38	$1.7 \times 10^{17}/n_H$
5 ...	1	1.15	0	0	13.8	$9.4 \times 10^{-20} n_H$	1.63	+0.31	$3.0 \times 10^{17}/n_H$
5 ...	1	1.10	0	0	51.1	$2.8 \times 10^{-19} n_H$	+7.88	+0.77	$1.8 \times 10^{17}/n_H$
10 ...	1	1.50	0	0.3	14.8	$6.8 \times 10^{-23} n_H$	+1.00	$+7 \times 10^{-4}$	$9.1 \times 10^{17}/n_H$
10 ...	1	1.50	0.25	0.3	35.5	$1.9 \times 10^{-21} n_H$	+39.6	-0.05	$(1.8 \times 10^{18}/n_H)$
10 ...	1	1.50	0.50	0.3	12.1	$5.3 \times 10^{-20} n_H$	+2.95	-0.03	$(5.4 \times 10^{17}/n_H)$
10 ...	1	1.075	0	0	33.5	$1.1 \times 10^{-20} n_H$	+61.6	+0.04	$2.2 \times 10^{17}/n_H$
10 ...	1	1.06	0	0	22.8	$7.0 \times 10^{-21} n_H$	+157.0	+0.02	$2.4 \times 10^{17}/n_H$
10 ...	2	3.00	0	0.3	10.5	$2.4 \times 10^{-22} n_H$	0	$+9 \times 10^{-4}$	$3.3 \times 10^{17}/n_H$
10 ...	2	3.00	0.25	0.3	20.3	$1.3 \times 10^{-20} n_H$	+15.5	-0.14	$(7.7 \times 10^{17}/n_H)$
10 ...	2	3.00	0.5	0.3	8.2	$1.3 \times 10^{-19} n_H$	+3.14	-0.27	$(1.9 \times 10^{17}/n_H)$
10 ...	2	2.30	0	0	33.3	$1.7 \times 10^{-20} n_H$	+0.05	+0.02	$6.7 \times 10^{16}/n_H$
10 ...	2	2.25	0	0	6.0	$3.1 \times 10^{-20} n_H$	+3.42	+0.03	$6.4 \times 10^{16}/n_H$
10 ...	2	2.20	0	0	8.3	$1.6 \times 10^{-19} n_H$	+0.97	+0.17	$6.0 \times 10^{16}/n_H$
10 ...	2	2.15	0	0	17.7	$1.8 \times 10^{-20} n_H$	+122	+0.02	$8.1 \times 10^{16}/n_H$

the angular momentum carried away by ejected material to the rotational angular momentum gained by the primary, per unit time interval. The transfer of angular momentum to the primary is mediated by particles only; dynamical or tidal friction are not directly included. Therefore, one should consider the values of R to be upper limits to this ratio. In order for these models to be applicable to BPNs, $|R|$ should be greater than about 0.1. In these numerical models, R can be negative, because in certain circumstances, the secondary can gain angular momentum at the expense of the primary's rotation. This happens because particles which are accelerated away from the primary surface can later merge with that surface with a much reduced angular momentum. It is not yet clear whether this mechanism can be important for binary star evolution in general or whether it can significantly impede the synchronization process

for close binaries; by delaying synchronization, it can only help the mass ejection process described here.

The time scale, τ , for the secondary to spiral inwards in each model (col. 10) is determined by dividing the secondary's angular momentum by the angular momentum loss rates due to the ejection of material and to the spinning up of the primary. τ is also expressed in terms of n_H . If τ is listed between parentheses, then it is the time scale for the secondary's angular momentum to double.

An inspection of Table 2 immediately shows two attractive features of the asynchronous binary model. First, the terminal velocities of the ejected matter conform quite well with those observed for BPNs. Second, in the models in which a significant fraction of the secondary's angular momentum has been lost to ejected material, a single value of n_H in the range 10^{14} to 10^{15}

cm^{-3} gives values for both the mass loss rate and the time scale, τ , which agree with those deduced for BPNs. Furthermore, densities in this range are those that are expected to occur near or above the photosphere of a red giant (e.g., Keeley 1970; Wood 1979). The required density of material at the original particle surface is thus well defined for these models. However, the surfaces of red giants are ill defined since dynamical processes probably act to levitate material to a distance of several pressure scale heights above the photosphere. This is an important point for the asynchronous binary model, since the time scale for synchronization by tidal friction varies with the sixth power of the binary separation (Alexander 1973). If the original particle surface of the models in Table 2 is not well above the photosphere (defined here as the radius below which most of the tidal friction takes place), then synchronization may occur rather quickly when M_p/M_s is substantially less than 6, and mass loss can then no longer occur by this mechanism. However, if the material which constitutes the original particle surface and which is ejected in the numerical models has been levitated to only 1.2–1.5 times the primary's photospheric radius, then the time scale for synchronization by tidal friction in the models is probably longer than the time scale for angular momentum loss by mass ejection. The levitation can be occasioned by the same processes that, carried to an extreme, give eventual rise to mass loss from solitary red giants (e.g., Wood 1974; Fusi-Peccì and Renzini 1975; Maciel 1976; Willson 1976; Willson and Hill 1979; Tuchman, Sack, and Barkat 1979). Of course, if the mass ratio is greater than 6, levitation is not required since the system cannot reach synchronism.

These considerations of the effect of an extended atmosphere motivated the inclusion of radial pulsation in some of the numerical models. As can be seen from Table 2, pulsation of modest amplitude permits the mass ejection to take place even though the binary separation is much greater than in the best models without pulsation. However, pulsation brings no unusually large mass loss rates. It can be regarded as one plausible means of mass levitation, but it is not a requirement for the model to work.

One advantage of the separated, asynchronous binary model over most of those discussed above is that it has the possibility of accounting for the latitudinal distribution of matter in BPNs. Although the numerical calculations presented in Table 2 were performed with the assumption of reflection symmetry about the equatorial plane, a realistic red giant probably deviates slightly from such a symmetry because of upwelling convection cells, prominences, etc. Therefore, although much of the gas crossing the midplane may undergo a strong shock as it meets its counterpart from the opposite hemisphere, a significant portion of the material pulled from the primary may pass relatively unhindered through the

midplane and thus be ejected at some intermediate latitude. Too little is known at the present time about the spectrum of asymmetries in red giants to warrant an attempt at deriving the latitudinal distribution of ejected matter. However, from the test calculations in which particles were not permitted to interact, it is clear that this mechanism is *not* effective at ejecting material at very high latitudes ($\sim 70\text{--}90^\circ$), which is consistent with the apparent cutoff of the dust density at high latitudes deduced in § II. In addition, the terminal velocity caused by this mechanism would not be a strong function of latitude, which is also consistent with the observational picture.

The shocks that are inferred to occur in the midplane are caused by gas streams that meet each other with relative velocities of $20\text{--}200 \text{ km s}^{-1}$, depending on the binary's mass ratio and separation. At the lower end of this velocity range, most molecules would be dissociated in the shock, and at the higher velocities, the material would be ionized and would emit ionizing radiation as it cooled.

In this model, shocks also occur in the outer envelope, although they are less strong than the midplane shock. Because of the above-mentioned asymmetries in the atmosphere of the primary, the ejection velocity in a given direction may vary from orbit to orbit over a range of about 10 km s^{-1} . Therefore, the faster gusts will overtake slower ones in the expanding envelope and create shocks which heat and compress the gas locally, although probably not to the extent of dissociating most of the molecules. The chemistry in the outer envelope shocks and in the cooling region downstream from the midplane shock is probably very rich and active and, if the asynchronous binary model is applicable, probably determines the abundances of the variety of molecules seen in BPN envelopes. The study of envelope chemistry, however, is beyond the scope of this paper.

The model for mass ejection presented here does not immediately explain the very high velocities ($400\text{--}600 \text{ km s}^{-1}$) evidenced in some BPNs by P Cygni profiles or wide emission lines. Such velocities *can* be achieved in binary systems of large mass at the point where the gas from the primary swings around the secondary on its way out of the system. However, the cross sectional area of the region occupied by the high velocity gas is much smaller than the primary's surface area, so that the depth of the P Cygni absorption feature would be expected to be much smaller than is observed. An appealing explanation for the systems displaying very high velocities is that when the hot core of the primary is exposed by the loss of its envelope, radiation pressure acting directly on gas at the surface of the stellar core causes a high velocity stellar wind to be set up. Observational evidence exists that such stellar winds are present in some planetary nebulae (Greenstein and Minkowski 1964; Smith and Aller 1969) and may play a role in

determining the structure of planetaries, starting from the early stages in which we are presumably seeing them in BPNs (Kwok, Purton, and FitzGerald 1978; Giuliani 1981).

IV. THE EVOLUTIONARY STATUS OF BIPOLAR NEBULAE

According to the binary model, the occurrence of a bipolar nebula corresponds to a stage in which the binary is rapidly losing angular momentum, and the secondary is thus doomed to spiral toward the primary. A common envelope binary is the unavoidable result unless the primary's atmosphere is completely ejected and/or transferred to the secondary before the two stars can merge. If a large fraction of the secondary's original angular momentum was lost to ejected material, then it is possible that corotation of the primary cannot be achieved even for mass ratios somewhat less than 6. Then, in the common envelope configuration, the secondary will quickly lose a substantial portion of its remaining angular momentum in the process of speeding up the rotation of the primary envelope through viscous drag.

On a time scale which is short compared to the expansion times of BPNs, the remainder of the envelope will be ejected soon after the common envelope configuration is reached (Paczynski 1976; Taam, Bodenheimer, and Ostriker 1978; Meyer and Meyer-Hofmeister 1979). The ensuing evolution of common envelope binaries has been discussed elsewhere (see Meyer and Meyer-Hofmeister 1979 and references therein), and so it will not be discussed at length here. As others have suggested, common envelope binaries (and, according to the arguments presented here, bipolar nebulae) are likely precursors of planetary nebulae, cataclysmic variables, and possibly some supernovae (Sparks and Stecher 1974). It is noteworthy in this regard that Zuckerman *et al.* (1976) suggested that the BPN GL 2688 is a preplanetary nebula on the basis of observational arguments which are entirely independent of those presented here.

The fact that O and B stars are found to be the central stars of many BPNs (Table 1) is consistent with this picture if we presume that these early-type stars are the cooling cores of the primaries whose envelopes have been entirely ejected. In those cases, the mass ejection process is finished and the outflowing envelope will become increasingly ionized by continued exposure to UV radiation as its inner boundary moves away from the central star. The large proportion of observed objects in this transitional stage between BPNs and planetary nebulae might be accounted for in part by the fact that a substantial ionized region makes them easier to notice in H α or other optical surveys. Young BPNs (like OH 231.8+4.2) can be extremely red, and thus they are

noticeable only by virtue of their infrared or molecular line radiation.

If the mass ejection terminates when the primary's envelope is entirely lost, then the ensuing ionization of the outflowing BPN by the remaining primary core will result in a toroidal distribution of high density ionized gas. That is, the highest density ionized gas, that in the equatorial plane, will have an inner boundary at the radius corresponding to the termination of mass ejection and an outer boundary at the radius where the H II region is ionization bounded. When the envelope expands to the extent that it becomes optically thin, then because the emissivity is proportional to the square of the density, the optical appearance will eventually be that of a ring shaped nebula. In this regard, it is extremely suggestive that a ring is a very common form for planetary nebulae (e.g., Aller and Liller 1968). For an object in the transitional stage between a BPN and a ring shaped nebula, one might expect to see the two lobes of the BPN appear to be connected by spatially continuous emission, such as appears to be the case with Mz 3 (Cohen 1977) or M 2-9 (Allen and Swings 1972).

According to the hypothesis presented here, the planetary nebula nucleus which results will be a binary, unless the ejection of the envelope requires the release of gravitational energy from the merger of the two stars. However, if the central star is a binary, the mass ratio may be large enough that the secondary's presence will be difficult to detect until the remaining core of the primary has cooled considerably. Even so, three close-binary planetary nebula nuclei are now known (Bond, Liller, and Mannery 1978; Bond, 1980; Drummond 1980), and their existence seems to require a prior stage of severe angular momentum loss such as would be the case with a common envelope binary (e.g., Paczynski 1976) and/or a BPN. It is probable that the fate of these objects is to become systems resembling V471 Tau (Vauclair 1972), PG 1413+01 (Green, Richstone, and Schmidt 1978), or Feige 24 (Thorstensen *et al.* 1978), and ultimately to become cataclysmic variables. Thus, bipolar nebulae may be an important key to the puzzle of how systems which are now cataclysmic variables have previously lost most of their angular momentum (Ritter 1976).

V. CONCLUSIONS

In this paper, I have presented models for the structure and for the origin of bipolar nebulae. The observed geometrical forms of BPNs can be accounted for on the basis of a simple condition—that the density of dust in the outflowing envelope decrease monotonically with latitude above the system's equatorial plane. A similar condition for the gas density can account for the OH maser line profiles observed in some BPNs. The origin of the outflow in BPNs can most satisfactorily be ex-

plained in terms of gravitational ejection from a close binary system in which the primary is a giant or a supergiant. The weakly bound outer layers of the primary's atmosphere are subject to removal by a closely orbiting secondary even if the mass ratio is large. An important condition for this ejection mechanism is that the primary not be corotating with the secondary's orbit. For binaries having mass ratios ≥ 6 , this condition is easily met. Systems having smaller mass ratios can also avoid synchronism if a large proportion of the original orbital angular momentum is lost to ejected material. After the primary's atmosphere has been removed, a BPN will be transformed into a planetary nebula which will probably have a binary central star. Much later, such systems are likely to become cataclysmic variables.

Obviously, one can test the binary hypothesis for BPNs by seeking evidence for the presence of close companions of their central stars. Unfortunately, this appears to be a difficult task for two reasons: (1) the primary's luminosity in its giant phase should overwhelm the light of the secondary even for small mass ratios, and (2) periodic velocity variations of the primary may be unobservable if the primary is obscured in all directions near the orbital plane; if the spectrum of the central star is discernible in reflection off dust only in directions which are nearly perpendicular to the orbital plane (i.e., the polar directions), then the component of the orbital velocity projected toward the observer will

probably be negligibly small unless some fraction of the light scattered in the polar reflection nebulae has previously been scattered by dust near the orbital plane close to the central object. Perhaps the best stage in which to search for a binary is in the transitional phase between BPNs and planetaries. Then, when the envelope becomes optically thin, one can view the central object directly from near the orbital plane. Interestingly, one BPN, the Red Rectangle, is a visual binary (Cohen *et al.* 1975), although its separation is ~ 100 times the separation of binaries considered here. In order to account for the mass outflow in the Red Rectangle with the mechanism I have suggested above, one is forced to invoke the presence of a third star in this system which is much closer to the central star than is the known visual companion.

For enlightening discussions and helpful suggestions, I am indebted to many of my colleagues, including Drs. L. Lucy, E. T. Scharlemann, N. Baker, K. Prendergast, B. Elmegreen, and M. Cohen. In addition, I am grateful to the astrophysical section of the Observatoire de Paris for supporting a visit during which some of this work was carried out and to the Goddard Institute for Space Studies in New York for use of their computational facilities. This research was supported in part by NSF grant 79-02601 to Columbia University.

APPENDIX

Further details of the numerical calculations of particle dynamics in a close, asynchronous binary system are presented here.

As described in § III, the particles are originally placed on the surface of a sphere and are initially given the velocity of the point on the rotating, orbiting sphere at which they are located. They are subsequently allowed to move according to the gravitational field in the binary. A further force, one which is analogous to the buoyancy of the atmosphere, is added in order to establish a well defined surface for the primary. It is a spherically symmetric, outward radially directed restoring force which is zero at a distance from the center of the primary equal to 1.01 of the radius of the particle surface, r_p , and which increases linearly with decreasing radius in such a way that it exactly balances gravity at r_p . This "buoyant" force continues to increase in the same linear fashion at radii smaller than r_p .

Deviations from sphericity may be important in close, asynchronous binaries (Kopal 1956; Plavec 1958; Kruszewski 1963; Limber 1963). This is to some extent taken care of in the present calculations by letting the particles move according to the imposed forces, although ideally the restoring force representing buoyancy should be refined to conform to the expected deviations

from sphericity. It is not anticipated that the spherically symmetric approximation used leads to any serious inaccuracies in the conclusions of this paper, especially in view of the essentially illustrative purpose of the calculations.

The initial separation between particles in the primary surface is specified in terms of their angular separation with respect to the center of the primary, and therefore the particle size depends on the primary's radius. For the models presented in Table 2, the particle diameters and initial separations were taken to be $\pi/35$ radians. When the imposed forces cause a particle to move away from its original site on the primary surface by more than 0.8 particle diameters, a new particle is created at the original, vacated site. As a result, the number of particles increases initially with time and in some circumstances may reach several thousand. Eventually, the proliferation of particles ceases as particles are eliminated at the same rate at which they are created.

A particle can be eliminated in three ways: (1) by achieving escape velocity from the system at a distance from the center of mass greater than five times the binary separation (see § III); (2) by hitting the surface of the secondary (see below); and (3) by following a trajectory which would carry it beneath the original particle

surface of the primary. This last condition applies only to particles which have previously left the surface and been replaced. When a particle is eliminated, the difference between its final and initial angular momenta is computed and stored so that the total loss of angular momentum and the transfer between stars can be determined.

For most of the calculations, the time step is taken to be 1/150 of the orbital period. During this time interval, particles near the secondary can undergo considerable change in their motion. Rather than use a smaller time step to get accurate trajectories near the secondary, we instead move a particle along a purely Keplerian orbit around the secondary whenever that particle is subject to a gravitational force from the secondary which is more than 40 times that from the primary. In addition, the Keplerian orbit is rotated about the secondary in each time step by the angle through which the binary rotates in a time step. If the periastron of a particle orbit about the secondary lies within the secondary, then that particle is assumed to have been assimilated by the secondary. In all models, the secondary radius is taken to be 5×10^{10} cm and is assumed not to change as a result of accretion. The mean terminal velocities and the mass loss rates are not greatly affected by changes in these assumptions, although this treatment is not expected to accurately represent mass accretion onto the secondary. In a realistic situation, the transfer of matter to the secondary would probably be mediated by an accretion disk. Since an accretion disk around the secondary has not been included in the model presented

here, one must regard the rates of mass transfer as crude estimates. A large accretion disk would increase the accretion rate, but the disk would have to be quite large ($\sim 10^{12}$ cm diameter) to inhibit mass ejection. Clearly, the ratio of mass ejected to mass exchanged does vary with the size of the secondary or its accretion disk.

The effect of radial pulsation of the primary was investigated in some models by varying the radius of the primary's original particle surface sinusoidally about its equilibrium value with half-amplitude δ (Table 2). This means in practice that (1) the radius at which the buoyant force appears is constrained to follow the radius of the particle surface, (2) the original particle positions move to follow the surface, and (3) the velocities of the original particle positions vary with time in such a way that the angular momentum of a particle following the surface is conserved. The period of a red giant pulsating in its fundamental radial mode is less than or on the order of the orbital period of a low mass secondary in a close orbit about the red giant. Because of the lack of further information about pulsation periods of giants, we simply assume in all the models presented here that the pulsational period of the primary is half of the orbital period of the binary. This assumption is not very important for the qualitative results of the models which include pulsation. If the pulsation period and the orbital period are indeed comparable in such a system, then it might be of interest to consider the possibility that the pulsation is driven by the varying gravitational field of the binary.

REFERENCES

- Alexander, M. E. 1973, *Ap. Space Sci.*, **23**, 459.
 Allen, D. A. 1978, *M.N.R.A.S.*, **184**, 601.
 Allen, D. A., Barton, J. R., Gillingham, P. R., and Phillips, B. A. 1980, *M.N.R.A.S.*, **190**, 531.
 Allen, D. A., Hyland, A. R., and Caswell, J. L. 1980, *M.N.R.A.S.*, **192**, 505.
 Allen, D. A., and Swings, J. P. 1972, *Ap. J.*, **174**, 583.
 Aller, L. H., and Liller, W. 1968, in *Nebulae and Interstellar Matter*, ed. B. M. Middlehurst and L. H. Aller (Chicago: University of Chicago Press), p. 483.
 Bond, H. E. 1980, *IAU Circ.* 3480.
 Bond, H. E., Liller, W., and Mannery, E. J. 1978, *Ap. J.*, **223**, 252.
 Calvet, N., and Cohen, M. 1978, *M.N.R.A.S.*, **182**, 687.
 Cohen, J. G., and Frogel, J. A. 1977, *Ap. J.*, **211**, 178.
 Cohen, M. 1977, *Ap. J.*, **215**, 533.
 Cohen, M., et al. 1975, *Ap. J.*, **196**, 179.
 Cohen, M., FitzGerald, M. P., Kunkel, W., Lasker, B. M., and Osmer, P. S. 1978, *Ap. J.*, **221**, 151.
 Cohen, M., and Kuhl, L. V. 1977, *Ap. J.*, **213**, 79.
 Crampton, D., Cowley, A. P., and Humphreys, R. M. 1975, *Ap. J. (Letters)*, **198**, L135.
 Davis, L. E., Seaquist, E. R., and Purton, C. R. 1979, *Ap. J.*, **230**, 434.
 Drummond, J. D. 1980, *Astr. Ap.*, **88**, L11.
 Flannery, B. P. 1977, 8th Texas Symp. on Relativistic Astrophysics, ed. M. D. Papagiannis, *Ann. NY Acad. Sci.*, **302**, 36.
 Flannery, B. P., and Ulrich, R. K. 1977, *Ap. J.*, **212**, 533.
 Fusi-Peccii, F., and Renzini, A. 1975, *Astr. Ap.*, **39**, 413.
 Giuliani, J. L. 1981, *Ap. J.*, **245**, 903.
 Glass, I. S., and Webster, B. L. 1973, *M.N.R.A.S.*, **165**, 77.
 Green, R. F., Richstone, D. O., and Schmidt, M. 1978, *Ap. J.*, **224**, 892.
 Greenstein, J. L., and Minkowski, R. 1964, *Ap. J.*, **140**, 1601.
 Harvey, P. M., and Lada, C. J. 1980, *Ap. J.*, **237**, 61.
 Herbig, G. H. 1975, *Ap. J.*, **200**, 1.
 Humphreys, R. M., Merrill, K. M., and Black, J. H. 1980, *Ap. J. (Letters)*, **237**, L17.
 Jones, T. J., and Dyck, H. M. 1978, *Ap. J.*, **220**, 159.
 Keeley, D. A. 1970, *Ap. J.*, **161**, 643.
 Kobayashi, Y., Kawara, K., Maihara, T., Okuda, H., Sato, S., and Noguchi, K. 1978, *Pub. Astr. Soc. Japan*, **30**, 377.
 Kopal, Z. 1956, *Ann. d'Ap.*, **19**, 298.
 Kruszewski, A. 1963, *Acta Astr.*, **13**, 106.
 Kuiper, G. P. 1941, *Ap. J.*, **93**, 133.
 Kwok, S., Purton, C. R., and FitzGerald, M. P. 1978, *Ap. J. (Letters)*, **219**, L125.
 Limber, D. N. 1963, *Ap. J.*, **138**, 112.
 Lo, K. Y., and Bechis, K. P. 1976, *Ap. J. (Letters)*, **205**, L21.
 Maciel, W. J. 1976, *Astr. Ap.*, **48**, 27.
 Manchester, R. N., Goss, W. M., and Robinson, B. J. 1969, *Ap. J. (Letters)*, **3**, 11.
 Meyer, F., and Meyer-Hofmeister, E. 1979, *Astr. Ap.*, **78**, 167.
 Milne, D. K., and Aller, L. H. 1975, *Astr. Ap.*, **38**, 183.
 Minkowski, R. 1946, *Pub. A.S.P.*, **58**, 305.
 Morris, M. 1980, *Ap. J.*, **236**, 823.
 Morris, M., and Bowers, P. F. 1980, *A. J.*, **85**, 724.
 Mufson, S. L., and Liszt, H. S. 1975, *Ap. J.*, **202**, 183.
 Ney, E. P., Merrill, K. M., Becklin, E. E., Neugebauer, G., and Wynn-Williams, C. G. 1975, *Ap. J. (Letters)*, **198**, L129.
 Paczynski, B. 1971, *Ann. Rev. Astr. Ap.*, **9**, 183.

- Paczynski, B. 1976, in *Structure and Evolution of Close Binary Systems*, ed. P. Eggleton et al. Dordrecht: Reidel.
- Pismis, P., and Hasse, I. 1980, preprint.
- Plavec, M. 1958, *Mém. Soc. Roy. Sci. Liège*, **20**, 411.
- Ritter, H. 1976, *M.N.R.A.S.*, **175**, 279.
- Roberts, M. S. 1962, *A. J.*, **67**, 79.
- Scharlemann, E. T. 1981, *Ap. J.*, in press.
- Schmidt, G. D., Angel, J. R. P., and Beaver, E. A. 1978, *Ap. J.*, **219**, 477.
- Schmidt, G. D., and Cohen, M. 1981, preprint.
- Schmidt, G. D., Cohen, M., and Margon, B. 1980, *Ap. J. (Letters)*, **239**, L133.
- Shaw, S. J. and Tarengi, M. 1976, *Ap. J. (Letters)*, **204**, L25.
- Shu, F. H., Lubow, S. H., and Anderson, L. 1979, *Ap. J.*, **229**, 223.
- Smith, L. F., and Aller, L. H. 1969, *Ap. J.*, **157**, 1245.
- Solf, J. 1980, *Astr. Ap.*, **92**, 51.
- Sparks, W. M., and Stecher, T. P. 1974, *Ap. J.*, **188**, 149.
- Stockton, A., Chesley, D., and Chesley, S. 1975, *Ap. J.*, **199**, 406.
- Taam, R. E., Bodenheimer, P., and Ostriker, J. P., 1978, *Ap. J.*, **222**, 269.
- Taylor, K. N. R., and Scarrott, S. M. 1980, *M.N.R.A.S.*, **193**, 321.
- Thorstensen, J. R., Charles, P. A., Margon, B., and Bowyer, S. 1978, *Ap. J.*, **223**, 260.
- Tuchman, Y., Sack, N., and Barkat, Z. 1979, *Ap. J.*, **234**, 217.
- Turner, B. E. 1971, *Ap. Letters*, **8**, 73.
- van den Bergh, S. 1974, *Astr. Ap.*, **32**, 351.
- Vauclair, G. 1972, *Astr. Ap.*, **17**, 437.
- Wegner, G., and Glass, I. S. 1979, *M.N.R.A.S.*, **188**, 327.
- Westbrook, W. E., Becklin, E. E., Merrill, K. M., Neugebauer, G., Schmidt, M., Willner, S. P. and Wynn-Williams, C. G. 1975, *Ap. J.*, **202**, 407.
- Willson, L. A. 1976, *Ap. J.*, **205**, 172.
- Willson, L. A., and Hill, S. J. 1979, *Ap. J.*, **228**, 854.
- Wood, P. R. 1974, *Ap. J.*, **190**, 609.
- _____ 1979, *Ap. J.*, **227**, 220.
- Zahn, J.-P. 1975, *Astr. Ap.*, **41**, 329.
- _____ 1977, *Astr. Ap.*, **57**, 383.
- Zuckerman, B., Gilra, D. P., Turner, B. E., Morris, M., and Palmer, P. 1976, *Ap. J. (Letters)*, **205**, L15.
- Zuckerman, B., Palmer, P., Gilra, D. P., Turner, B. E., and Morris, M. 1978, *Ap. J. (Letters)*, **220**, L53.
- Zuckerman, B., Palmer, P., Morris, M., Turner, B. E., Gilra, D. P., Bowers, P. F., and Gilmore, W., 1977, *Ap. J. (Letters)*, **211**, L97.

MARK MORRIS: Department of Astronomy and Astrophysics, Box 98, Pupin Labs, Columbia University, New York, NY 10027